Journal of Materials Chemistry C

Accepted Manuscript

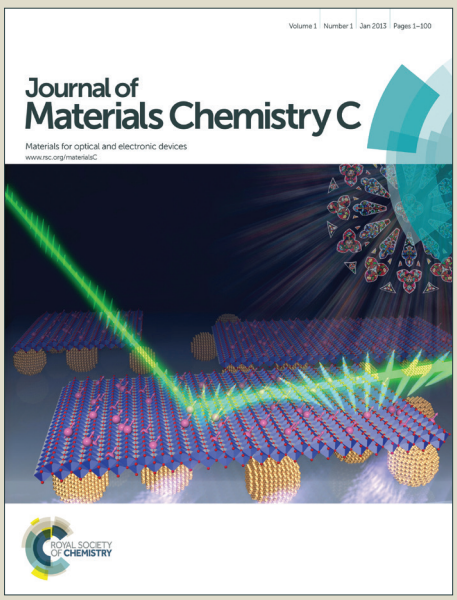

This is an *Accepted Manuscript*, which has been through the Royal Society of Chemistry peer review process and has been accepted for publication.

Accepted Manuscripts are published online shortly after acceptance, before technical editing, formatting and proof reading. Using this free service, authors can make their results available to the community, in citable form, before we publish the edited article. We will replace this *Accepted Manuscript* with the edited and formatted *Advance Article* as soon as it is available.

You can find more information about *Accepted Manuscripts* in the Information for Authors.

Please note that technical editing may introduce minor changes to the text and/or graphics, which may alter content. The journal's standard Terms & Conditions and the Ethical guidelines still apply. In no event shall the Royal Society of Chemistry be held responsible for any errors or omissions in this *Accepted Manuscript* or any consequences arising from the use of any information it contains.

ROYAL SOCIETY OF CHEMISTRY

www.rsc.org/materialsC

Journal of Materials Chemistry C

Cite this: DOI: 10.1039/c0xx00000x

www.rsc.org/xxxxxx

PAPER

Resonance energy transfer-enhanced rhodamine-styryl bodipy dyad triplet photosensitizers

Jie Ma,[a,b‡] Xiaolin Yuan,[c‡] Betül Küçüköz,[d] Shengfu Li,[c] Caishun Zhang,[a] Poulomi Majumdar,[a] Ahmet Karatay,[d] Xiaohuan Li,[c] H. Gul Yaglioglu,[d] Ayhan Elmali,[d] Jianzhang Zhao[a]* and Mustafa Hayvali [e]*

Received (in XXX, XXX) Xth XXXXXXXXX 20XX, Accepted Xth XXXXXXXXX 20XX
DOI: 10.1039/b000000x

Organic triplet photosensitizers (**R-1** and **R-2**) enhanced with resonance energy transfer (RET) effect were prepared. Rhodamine was used as intramolecular energy donor and iodo-styryl Bodipy was used as intramolecular energy acceptor/spin converter. Both the energy donor and the energy acceptor in **R-1** and **R-2** give strong absorption in visible region, but at different wavelength (e.g. for **R-1**, $\varepsilon = 120000$ M^{-1} cm^{-1} at 557 nm for the energy donor, and $\varepsilon = 73300$ M^{-1} cm^{-1} at 639 nm for the energy acceptor). As a result the photosensitizers show *broadband* absorption in visible spectral region. In comparison, the conventional triplet photosensitizers contain only one visible light-harvesting chromophore, thus there is usually only one major absorption band in visible spectral region. With steady state and time-resolved spectroscopy, we demonstrated that photoexcitation into the energy donor was followed by intramolecular singlet energy transfer, then via the intersystem crossing (ISC) of the energy acceptor (spin converter), triplet excited states localized on the iodo-styryl-Bodipy were produced, confirmed by nanosecond time-resolved transient difference absorption spectroscopy. The organic dyad triplet photosensitizers were used for photoredox catalytic organic reactions to prepare pyrrolo[2,1-*a*]isoquinoline and we found that the photocatalytic capability was improved with the RET effect. The dyads were used as fluorescent stains for LLC cancer cells. Photodynamic effect was observed with the same cells, which were killed upon photoirradiation with 635 nm red emitting LED after incubation with the triplet photosensitizers. Therefore these photosensitizers can be potentially developed as dual functional theranostic reagents. With the molecular structural protocol reported herein, organic triplet photosensitizers with strong *broadband* absorption in visible spectral region and *predictable* ISC can be easily designed. These results are useful for study of organic triplet photosensitizers in the area of organic photochemistry/photophysics, photoredox catalytic organic reactions and photodynamic therapy (PDT).

Introduction

Recently triplet photosensitizers have attracted much attention, owing to the applications in photodynamic therapy (PDT),[1–7] photosensitizing of singlet oxygen ($^1O_2$),[6,8–10] photoredox catalytic organic reactions,[11–15] photocatalytic hydrogen (H_2) production,[16–19] and triplet-triplet annihilation upconversions.[20–23] Triplet photosensitizers are the compounds with triplet excited state being produced upon photoexcitaion.[1-7] Fluorescent dyes alone are not applicable to the aforementioned applications, because the production of the triplet excited state yield by these compounds upon photoexcitation is inefficient.[1,5,7,24] Thus, design of triplet photosensitizers with high triplet excited state yield, or efficient intersystem crossing (ISC), is crucial.[7]

On the other hand, different from the fluorescent dyes, for which the main application is luminescence, triplet photosensitizers are usually involved in triplet energy transfer or electron transfer.[7,25,26] Accordingly, an ideal triplet photosensitizer should be with the following photophysical properties, (1) strong absorption of visible light, or more preferably *broadband* absorption in visible spectra; (2) long-lived triplet excited states, so that the intermolecular triplet-triplet-energy-transfer (TTET) and electron transfer can be enhanced; (3) tunable molecular structures so that the photophysical and redox properties can be readily optimized. Unfortunately, investigations on triplet photosensitizers are rare and the above challenges are left to overcome.[5,24]

Conventional triplet photosensitizers include the porphyrin derivatives, aromatic ketones, iodo- or bromo-organic chromophores, such as Bodipy, or the transition metal complexes contain Pt(II), Ir(III) or Ru(II) atoms.[7] While widely used, these triplet photosensitizer still suffer from some drawbacks, such as high cost, difficulties to modify the molecular structure or to prepare and purify the compounds. Furthermore, all these conventional triplet photosensitizers share a common molecular structural protocol, that is, there is only *one* kind of visible light-harvesting chromophore in these compounds. As a result, these compounds show only one major absorption band in the visible

Journal of Materials Chemistry C Accepted Manuscript

spectral region.[1–7] This is a clear disadvantage if a panchromatic light source was used for photoexcitation, such as solar light. Moreover, it is difficult to design new triplet photosensitizers especially those containing no heavy atoms.[7] Subtle alternation of the molecular structures of an organic chromophore may eliminate the ISC property completely. In order to prepare triplet photosensitizers that show predictable ISC efficacy, one strategy is to use an intramolecular spin converter.[7] But this strategy was rarely used for construction of organic triplet photosensitizers.

Previously C_{60} was used as such spin converter in dyad triplet photosensitizers.[7,25,27,28] C_{60} shows efficient ISC but very weak absorption in visible spectral region (ε < 2000 M^{-1} cm^{-1} in the region > 400 nm), hence a dyad of C_{60} with visible light-harvesting chromophore cannot be used for construction of triplet photosensitizers that show broadband absorption. Recently we reported Bodipy-iodo-Bodipy dyad triplet photosensitizers, however, the intramolecular energy donor and the energy acceptor show similar absorption wavelength, thus the absorption band is still 'narrow'.[29a] Recently we prepared styryl Bodipy-iodo aza-Bodipy triad triplet photosensitizers which show broadband absorption of visible light.[29b] But much room is left for exploring other chromophores for construct broadband absorbing triplet photosensitizers.

In order to overcome the above challenges in the designing of triplet photosensitizers, herein we designed a resonance energy transfer (RET)-based organic triplet photosensitizers, in which Rhodamine chromophore is used as visible light-harvesting energy donor, the iodo-styryl-Bodipy as energy acceptor, and at the same time, the intramolecular spin converter.[7,29] Both Rhodamine and the Bodipy units show strong absorption of visible light, but at different wavelength. As a result, the Rhodamine/iodo styryl Bodipy dyad triplet photosensitizers show *broadband* absorption in the visible spectral region, and *predictable* ISC.

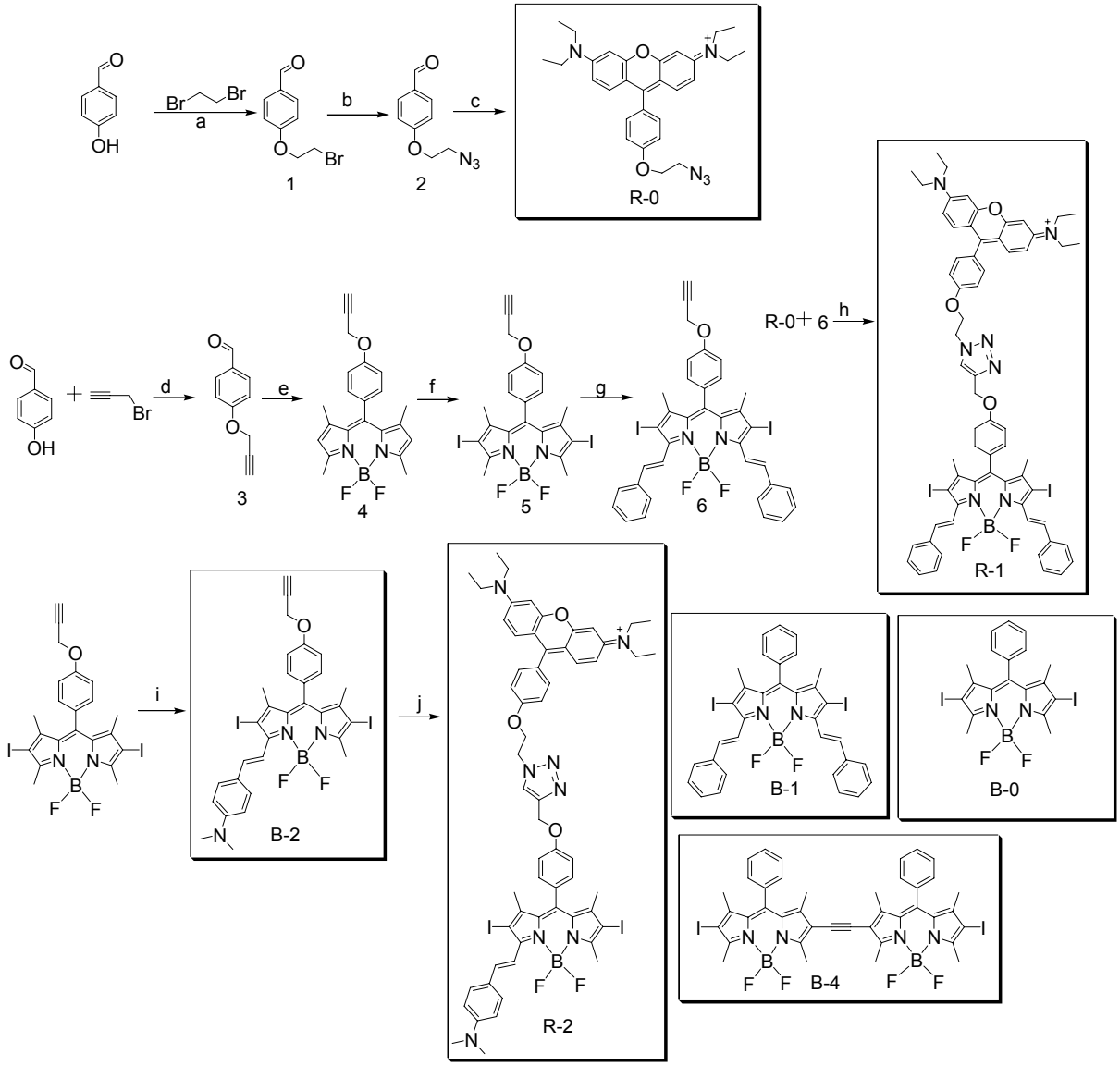

Scheme 1. Preparation of the RET triplet photosensitizer **R-1** and **R-2**.[a] **Key**: (a) K_2CO_3 and DMF, reflux, 6 h. (b) DMF, 100 °C, 2 h. (c) 3-(diethylamino)phenol, *p*-TsOH, 70 °C. (d) K_2CO_3 and DMF, reflux, 6 h. (e) nitrogen condition, CH_2Cl_2, TFA, DDQ, Et_3N and $BF_3{\cdot}Et_2O$. (f) NIS and CH_2Cl_2, r.t., 5 h. (g) benzaldehyde, acetic acid and piperidine, microwave irradiation. (h) $CuSO_4{\cdot}5H_2O$, Sodium ascorbate. 24 h. (i) *p*-*N*,*N*-dimethylamino-benzaldehyde, acetic acid and piperidine, microwave irradiation. (j) $CuSO_4{\cdot}5H_2O$, Sodium ascorbate. 24 h.

This journal is © The Royal Society of Chemistry [year]

Journal of Materials Chemistry C Accepted Manuscript

With steady state and time-resolved spectroscopy, as well as DFT calculations, we proved that upon photoexcitation, intramolecular energy transfer occurred for the dyad triplet photosensitizers and the triplet excited state localized on the iodo-styryl-Bodipy part was produced following the ISC of the spin converter. The dyad triplet photosensitizers were used as photocatalysts in photoredox catalytic organic reactions and we proved that the photocatalytic ability of the dyad triplet photosensitizer was improved as compared with the reference triplet photosensitizer which contains only one visible light-harvesting chromophore. With fluorescence confocal microscopy we found that the dyad triplet photosensitizers can enter cytosol of LLC cancer cells. Photodynamic effect was observed with the dyad triplet photosensitizers, that is, the LLC cells were killed upon photoirradiation with 635 nm red-emitting LED after incubation with the photosensitizers. Thus the photosensitizers can be developed as theranostic reagents. These results are useful for the designing of new triplet photosensitizers and the application of these compounds in the area of photocatalysis, solar cell and PDT.

Results and Discussion

Design and synthesis of the triplet photosensitizers

The principle molecular designing rationales are (1) using two different visible light-harvesting chromophores which give drastically different absorption wavelength to achieve *broadband* absorption; (2) singlet energy transfer (RET) occur from one chromophore to another one; (3) efficient ISC at the singlet energy acceptor to ensure production of triplet excited state upon photoexcitation. Previously we reported dyad triplet photosensitizers with unsubstituted Bodipy used as energy donor and iodo-Bodipy was used as energy acceptor.[29a] However, those triplet photosensitizers show relatively narrow absorption band in the visible region because the two chromophores show absorption band close to each other. In order to broaden the absorption band of the dyad triplet photosensitizer, herein Rhodamine was selected as the one of the visible light harvesting moiety (λ_{abs} = 556 nm) and the energy donor. Iodo-styryl-Bodipy as the energy acceptor (λ_{abs} = 640 nm), and at the same time, the spin converter (**R-1** and **R-2**, Scheme 1).[7,29] The two moieties were connected together by the Cu(I)-catalyzed azide alkyne Huisgen cycloaddition (Click reaction).

Rhodamine shows strong absorption in visible region and was extensively used in fluorescence studies (related to singlet excited states), such as FRET dyads,[30–33] but its application in *triplet* excited state manifold is very rare.[34] To the best of our knowledge, Rhodamine has not been used for construction of RET triplet photosensitizers.[29] Normally rhodamine is in the non-fluorescent tautomer of lactam in aprotic solvents, which also show very weak absorption in visible region. In order to avoid this complexity, we prepared a rhodamine compounds which is devoid of the –COOH group (**R-0**, Scheme 1). The simple synthetic procedure may be useful for preparation of new rhodamine derivatives.

Rhodamine shows absorption at 556 nm and emission at 575 nm. In order to construct efficient FRET molecular array, styryl-Bodipy **B-1** and **B-2** were selected as the energy acceptor, which gives absorption at 637 nm, so that there is substantial overlap between the emission of Rhodamine and the absorption spectrum of the iodo-styryl Bodipy (Scheme 1). Iodo-substitution was introduced at the 2,6-position of the π-system of the energy acceptor Bodipy to maximize the ISC effect, because the ISC of the Bodipy chromophore without any heavy atom is non-efficient.[1,3,5,24,35–37] The energy donor and the energy acceptor modules in **R-1** can be easily changed to different structures, which was demonstrated by the preparation of **R-2** (Scheme 1). All the preparation was based on established synthetic protocols and the compounds were obtained in satisfactory yields (Scheme 1 and experimental section).

UV-Vis absorption spectra and fluorescence spectra

The UV-Vis absorption spectra of the compounds were studied (Fig. 1). The energy donor **R-0** shows strong absorption at 556 nm (ε = 85000 M^{-1} cm^{-1}). The energy acceptor **B-1** shows absorption at longer wavelength of 637 nm (ε = 93600 M^{-1} cm^{-1}). The light-harvesting profiles of the typical mono-chromophore compounds can be demonstrated by **R-0** and **B-1**, i.e. they show only *one* major absorption band in the visible region. On the contrary, the dyad **R-1** shows strong absorption at both 557 nm and 639 nm. The UV-Vis absorption spectrum of **R-1** is superimposable to the sum of the absorption spectra **R-0** and **B-1** (Fig. 1a). Therefore the electronic interaction of the energy donor and the energy acceptor in **R-1** is weak at ground state.[33,38-42] Notably **R-1** shows strong broad absorption in the region of 500 – 700 nm. Similar absorption profiles were observed for **R-2** (Fig. 1b). **B-2** shows broad absorption at 639 nm, which is slightly different from **B-1**.

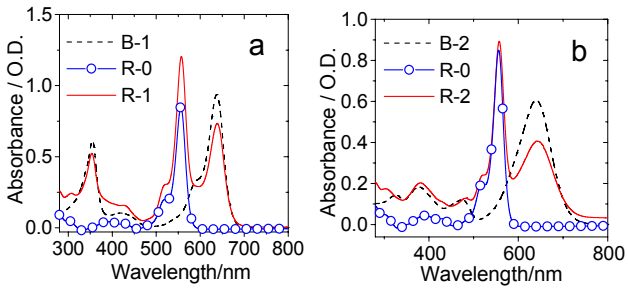

Fig. 1 UV-vis absorption of (a) **B-1**, **R-1** and **R-0** (b) **B-2**, **R-2** and **R-0**. $c = 1.0\times10^{-5}$ M in CH_2Cl_2, 20 °C.

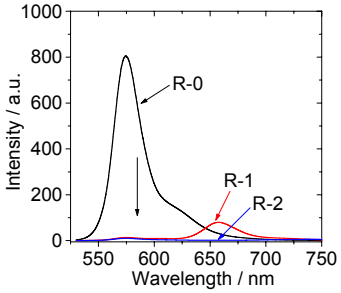

Fig. 2 Emission spectra of **R-0**, **R-1** and **R-2** (λ_{ex}= 520 nm, at which the three samples show the same absorbance A = 0.18. The concentration of the solutions is slightly different). In CH_2Cl_2. 20 °C.

Journal of Materials Chemistry C Accepted Manuscript

In order to evaluate the intramolecular energy transfer in **R-1** and **R-2**, the fluorescence spectra of the compounds were studied (Fig. 2. The solutions are with same optical density at the excitation wavelength). **R-0** gives strong fluorescence emission at 575 nm (Φ_F = 43 %). However, this intense emission was completely quenched in **R-1** and **R-2** (Fig. 2). This significant quenching effect demonstrated the intramolecular energy transfer from the singlet excited state of rhodamine to the styryl Bodipy unit.[33,38-41,43,44] We studied the fluorescence emission of the mixture of **R-0** and **B-1**, no quenching effect on the emission of **R-0** was found (Figure S36), thus the RET effect in **R-1** can be confirmed.

Quenching of the fluorescence of energy donor does not gurantee intramolecular energy transfer because electron transfer can also induce quenching.[39,40,45,46] Thus, the fluorescence of **B-1** was compared with that of **R-1**, upon selective excitation into the energy accetpor. Similar emission intensity was observed (Fig. 3a). For **R-2**, however, the emission intensity is smaller as compared with that of **B-2** (Fig. 3b). These results indicated that the electron transfer in the dyads are not significant.

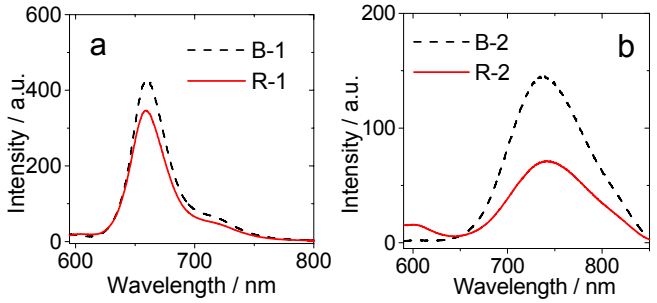

Fig. 3 Emission spectra of (a) **B-1** and **R-1** (λ_{ex}=585 nm, at which $\varepsilon_{B\text{-}1}$ =$\varepsilon_{R\text{-}1}$ =30000 M^{-1} cm^{-1}); (b) **B-2** and **R-2** (λ_{ex}=581 nm, $\varepsilon_{B\text{-}2}$ = $\varepsilon_{R\text{-}2}$ = 24000 M^{-1} cm^{-1}). c = 1.0 × 10^{-5} M in CH_2Cl_2. 20 °C.

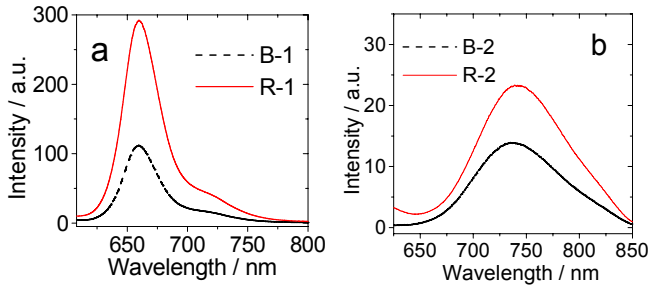

Fig. 4 Emission of the compounds upon excitation at the energy donor. (a) **B-1** and **R-1** (λ_{ex}= 557 nm; at which $\varepsilon_{B\text{-}1}$ = 10200 M^{-1} cm^{-1}, $\varepsilon_{R\text{-}1}$ = 121000 M^{-1} cm^{-1}); (b) **B-2** and **R-2** (λ_{ex}= 557 nm; at which $\varepsilon_{B\text{-}2}$ = 11400 M^{-1} cm^{-1}, $\varepsilon_{R\text{-}2}$ = 89400 M^{-1} cm^{-1}). c = 1.0 × 10^{-5} M in CH_2Cl_2, 20 °C.

The fluorescence emission of the dyads was also recorded by selectively excitation at the absorption of the energy donor (Fig. 4). The dyad gives much stronger absorption at the energy donor absorption band, than the energy acceptor alone (Fig. 1). On the other hand, the emission of the energy acceptor in the dyads will not be enhanced without the intramolecular energy transfer, even the dyads give stronger absorption at the energy donor band position. For **R-1**, the emission of the energy acceptor is much stronger than that of the reference compound **B-1** when excited at the same wavelength (Fig. 4a). Thus, we propose there is intramolecular energy transfer from the rhodamine moiety to the iodo-styryl-Bodipy unit in **B-1**. Similar results were observed for **R-2**, but the enhancement of the fluorescence emission is to a much less extent (Fig. 4b).

The photophysical properties of the compounds were summarized in Table 1. The photophysical properties of the compounds in different solvents were studied. Normally the compounds give hypochromatic shift in polar solvent as compared with that in apolar solvent. For the fluorescence emission, **B-2** and **R-2** show red-shifted emission band in polar solvent, such as CH_3CN. These results indicated more significant intramolecular charge transfer (ICT) in **B-2**.

Table 1. Photophysical Properties of **R-1, R-2, R-0, B-1** and **B-2** [a]

	Solvents	λ_{abs} [b]/nm	ε [c]	λ_{em} [d]/nm	τ [e]/ns	Φ_Δ [h]	Φ [i]%	τ_T [f](μs)	
								air	*Ar*
R-1	$PhCH_3$	551	52700	659	1.66	– [j]	8.6	0.15	1.64
		641	67400						
	DCM	557	120000	660	1.89	0.738 [k]	9.0	0.29	1.53
		639	73300			0.524 [m]			
	CH_3CN	554	106600	653	1.41	– [j]	4.6	0.14	1.46
		631	60800						
R-2	$PhCH_3$	552	29400	698	1.93	– [j]	5.8	0.18	3.29
		643	39100						
	DCM	557	89400	739	1.37	0.396 [k]	4.2	0.36	4.09
		641	40600			0.087 [m]			
	CH_3CN	555	78000	577	– [g]	– [j]	– [g]	0.14	4.19
		633	35200						
R-0	$PhCH_3$	564	14700	584	1.49	– [j]	22.8	– [g]	– [g]
	DCM	556	85000	575	4.19	– [j]	43.0	– [g]	– [g]
	CH_3CN	554	81800	579	1.60	– [j]	34.0	– [g]	– [g]
B-1	$PhCH_3$	643	103400	663	1.93	– [j]	11.1	0.15	1.73
	DCM	637	93600	660	1.84	0.624 [k]	10.1	0.28	1.80
	CH_3CN	629	90400	655	1.73	– [j]	9.9	0.12	1.26
B-2	$PhCH_3$	647	77900	706	1.88	– [j]	0.8	0.17	3.48
	DCM	639	60600	738	1.57	0.585 [k]	3.4	0.31	3.95
	CH_3CN	630	59900	– [g]	– [g]	– [j]	– [g]	– [g]	4.47

[a] The excited wavelength for **R-1, R-2, R-0, B-1** and **B-2** were 520 nm, 520 nm, 520 nm, 600 nm and 600 nm respectively (1.0 × 10^{-5} M, 20 °C). [b] Absorption wavelength. [c] Molar extinction coefficient. In $M^{-1}cm^{-1}$. [d] Fluorescence emission wavelength. [e] Fluorescence lifetimes. [f] Triplet state lifetimes. [g] No signal. [h] Quantum yield of singlet oxygen ($^1O_2$). [i] Fluorescence quantum yields with **B-4** as the standard. [j] Not determined. [k] With methylene blue (MB) as standard (Φ_Δ= 0.57 in CH_2Cl_2, λ_{ex}=580 nm). [m] With **B-0** as standard (Φ_Δ= 0.83), λ_{ex}=543 nm for **R-1** and λ_{ex} = 545 nm for **R-2**.

Recently, fluorescence excitation spectra were used for evaluation of the intramolecular energy transfer in FRET molecular arrays.[40] The fluorescence excitation spectra of **R-1** and **R-2** were compared to the UV-Vis absorption spectra (Fig. 5). The excitation at the energy donor is less efficient to produce the fluorescence of energy acceptor. The values of the intramolecular energy transfer efficiency was calculated as 56.3% and 53.2 %,

Journal of Materials Chemistry C Accepted Manuscript

This journal is © The Royal Society of Chemistry [year]

respectively (calculated by the intensity ratio of the excitation and the absorption spectra, at the donor absorption peak wavelength).[40] These values are comparable to the intramolecular energy transfer efficiencies in FRET molecular arrays.[40]

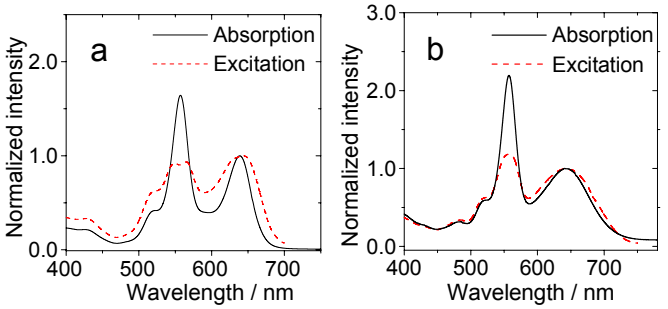

Fig. 5 Normalized UV-Vis absorption and excitation spectra: (a) **R-1**, λ_{ex} = 700 nm; (b) **R-2**, λ_{ex} = 750 nm. $c = 1.0 \times 10^{-5}$ M in CH_2Cl_2, 20 °C.

Nanosecond time-resolved transient different absorption spectra: population of the triplet excited states

In order to prove the generation of the triplet excited states of the triplet photosensitizers upon photoexcitation, the nanosecond time-resolved transient difference absorption spectroscopy were studied (Fig. 6).[7,25,27,28,36] Upon pulsed laser excitation at 532 nm, bleaching band at 630 nm was observed for **R-1** (Fig. 6a), where the iodo-styryl-Bodipy gives the steady state absorption. Furthermore, positive absorption at 390 nm, 514 nm and in the region of 650 – 800 nm were observed. These features are attributed to the triplet excited state absorption of styryl-Bodipy.[27,42] The lifetime of the transient was determined as 1.53 μs in deaerated solution. In aerated solution, however, the lifetime was substantially reduced to 0.29 μs. The lifetime of **R-1** is close to that of **B-1** (1.80 μs), and the transient feature of **R-1** is similar to **B-1** (Fig. 6c). These results indicated that the transients observed for **R-1** is due to the triplet excited state, which is

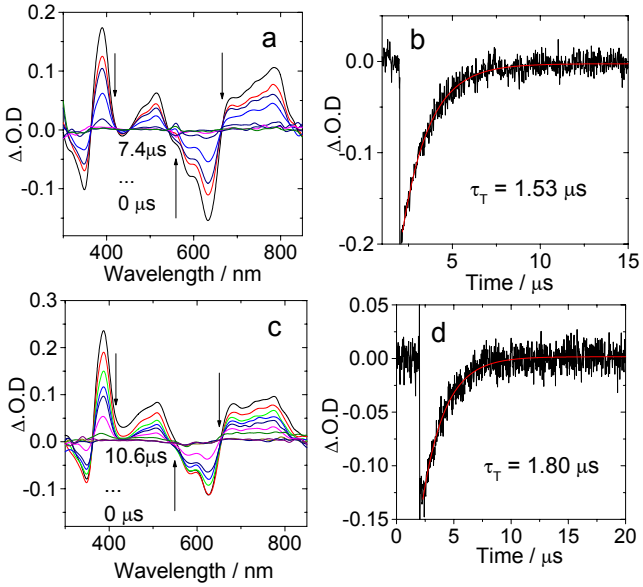

Fig. 6 Nanosecond time-resolved transient difference absorption of (a) **R-1** and (c) **B-1** after pulsed laser excitation (λ_{ex} = 532 nm). Decay trace of (b) **R-1** and (d) **B-1** at 630 nm. $c = 1.0 \times 10^{-5}$ M in deaerated CH_2Cl_2. 20 °C.

localized on the iodo-styryl-Bodipy unit, not the rhodamine unit.[25,27] The selective localization of the triplet excited state (T_1 state) of **R-1** is due to the lower energy level of the T_1 state of the iodo-styryl-Bodipy unit (1.13 eV) as compared with the T_1 state of the rhodamine unit (1.72 eV).

Similar results were observed for **R-2** (See ESI † Fig. S41). The triplet excited state of **R-2** shows a lifetime of 4.09 μs, which is close to that of the reference compound **B-2** (3.95 μs). Interestingly, these triplet excited state lifetimes of styryl Bodipy are much shorter than that observed in styryl Bodipy-C_{60} dyads (up to 123.2 μs).[27] We propose the different triplet excited state lifetime is due to the presence of iodo-substituent on the styryl-Bodipy unit in **R-1** and **R-2**. Direct attachment of the iodo atoms to the π-system is essential for efficient ISC. However, this efficient ISC may reduce the lifetime of the triplet excited state.[47]

In order to study intramolecular electron transfer, the redox potentials of the triplet photosensitizers were studied (see ESI † Fig. S35).[42,45,48–50] Calculation of the free energy changes of the electron transfer show that electron transfer is possible at the singlet excited state of the energy donor, which is similar to the results of Bodipy-C_{60} dyad (see ESI †for detail calculations).[45]

DFT Calculations: intramolecular energy transfer and localization of the T_1 states.

In order to study the localization of the triplet excited states of the dyads from a theoretical perspective, the spin density surfaces of the dyads triplet photosensitizers and the reference compounds were calculated with the density functional theory (DFT) (Fig. 7).[7,51-56] For the reference compounds **B-1** and **B-2**, the spin density surface was fully spread on the π-system of the chromophore. The meso phenyl rings of **B-1** and **B-2** were not involved in the spin density surface. For rhodamine **R-0**, similar results were observed. However, the meso phenyl ring is more involved in the spin density surface (see ESI† Fig. S53).

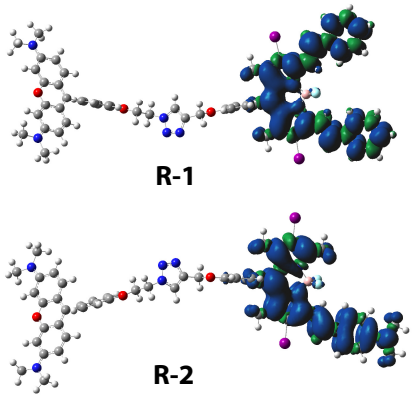

Fig. 7 Isosurfaces of spin density of compounds **B-1**, **B-2, R-0, R-1 and R-2**. At the optimized triplet state geometries. DCM was used as solvents in the calculations. Calculation was performed at B3LYP/6-31G(d)/genecp level with Gaussian 09W. .

The spin density surfaces of the dyad triplet photosensitizers **R-1** and **R-2** are localized on the styryl Bodipy units (Fig. 7). The rhodamine unit does not contribute to the spin density surfaces. Therefore, we propose that the triplet state of **R-1** and **R-2** are highly localized on the strytyl Bodipy moiety.[28,29,57-59] This conclusion is in full agreement with the nanosecond time-

Journal of Materials Chemistry C Accepted Manuscript

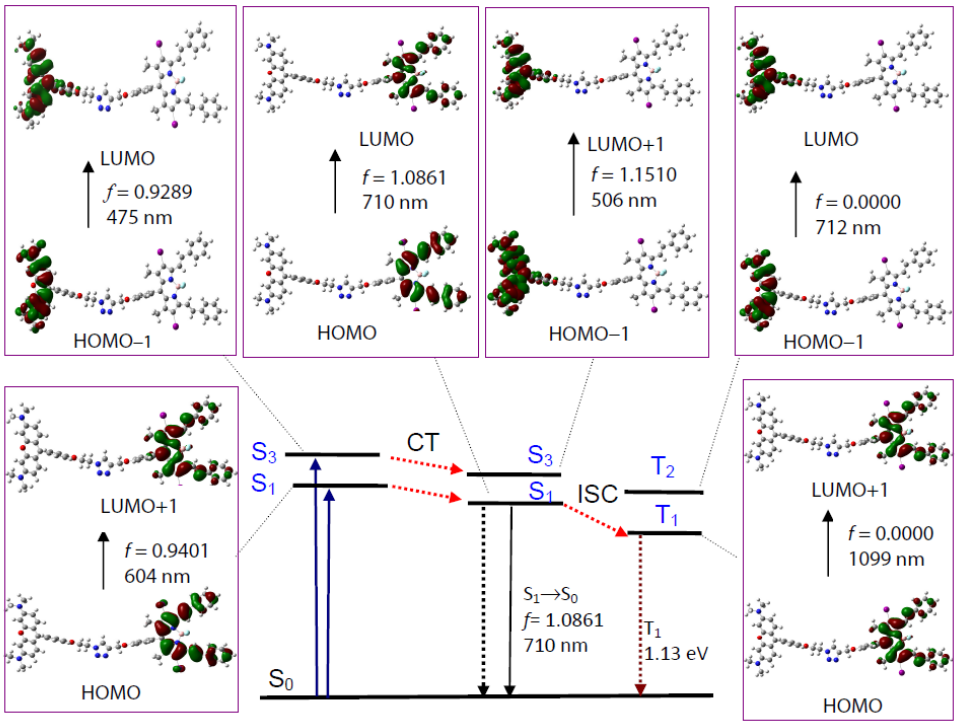

Fig. 8 Selected frontier molecular orbitals involved in the excitation, emission and triplet excited states of **R-1**. CT stands for conformation transformation. The calculations are at the TDDFT/B3LYP/6-31G(d)/Genecp level using Gaussian 09W. DCM was employed as solvent in the calculation.

resolved transient absorption spectroscopy of the dyad triplet photosensitizers (Fig. 6 and ESI †, Fig. S37 and S38).

The ground state geometries of the compounds were studied. The result shows that the Rhodamine and the iodo-styryl Bodipy moieties keep far away from each other, for which the steric hindrance exerted by the Rhodamine and the iodo-styryl Bodipy parts is minimal. This result is in agreement with the steady state and the time-resolved spectroscopic studies, that is, there is no significant interaction for the two chromophores at ground state and the excited states.

Time-dependent DFT was used for study of the excited states of the dyad triplet photosensitizers.[44,53,60-64] For **R-1**, two low-lying singlet excited states were indentified for **R-1**, i.e. S_1 and S_3 state, with absorption maximum at 604 nm and 475 nm, respectively (see ESI †, Table S4). Inspection of the molecular orbitals indicated that transitions are localized on the iodo-styryl Bodipy part and the Rhodamine part, respectively. This result is in agreement with the absorption bands of **R-1** (Fig. 1).[44]

A charge transfer state is also indentified (S_2 state), which is at 2.09 eV (594 nm). S_2 state is a dark state ($f = 0$). Since this charge transfer state is not the lowest-lying state, we propose the photophysical properties of **R-1** will be hardly affected by this state. This postulation is in agreement with the fluorescence lifetime of **R-1**.

The geometries of the singlet excited states were also optimized with the TDDFT method, and the fluorescence of **R-1** was calculated. The fluorescence emission of **R-1** is predicted as 710 nm, which is close to the experimental result (660 nm). The orbitals involved in S_1 state is localized on the iodo-styryl Bodipy part (Fig. 8). S_3 state is identified as an excited state localized on Rhodamine. According to Kasha's rule, however, this state will not fluoresce. Therefore, the internal conversion will funnel the energy from the S_3 state to S_1 state. This senario is in full agreement with the conventional FRET concept.[44]

The triplet states of **R-1** were also studied with TDDFT calculations, based on the optimized ground state geometry.[65] T_1 state is identified as localized on the iodo-styryl-Bodipy part, T_2 state was localized on the Rhodamine part. The energy difference of the T_1 and T_2 state is 0.61 eV (Fig. 8 and Table S4). Therefore, triplet excited state equilibirum was not observed.[29a]

Femto-second transient absorption spectroscopy

Ultrafast pump probe experiments were performed for both **R-1** and **R-2** at 555 nm and 640 nm pump wavelengths to excite the Rhodamine and iodo-styryl-Bodipy units, respectively.[39] Pump pulse at 555 nm excites the Rhodamine ($S_0 \rightarrow S_1$). It is expected ultrafast spectroscopy results give the evidence of singlet state intramolecular energy transfer and formation of triplet state of iodo-styryl-Bodipy units in **R-1** (Fig. 9). The bleaching signals around 560 nm and 640 nm were observed upon femtosecond pulsed laser excitation at 555 nm, where the Rhodamine give the steady state absorption, respectively. Energy transfer may be responsible for the decay of the bleaching band of **R-1**.[39] On the other hand, while the bleaching signal around 560 nm decreases, the second bleaching signal around 640 nm slightly increases for **R-1**. Based on the steady state UV-Vis absorption spectra, the Bodipy part will also be excited with the 555 nm pump, therefore the singlet state of the Bodipy part can be generated by the direct photoexcitation. Energy transfer from the Rhodamine part contributes partially to the production of the singlet excited state of the Bodipy part.[39] Similar results were observed for **R-2** (see ESI † Fig. S45).

The kinetics of the singlet energy transfer in **R-1** upon photoexcitation were followed by monitoring the transient

Journal of Materials Chemistry C Accepted Manuscript

This journal is © The Royal Society of Chemistry [year]

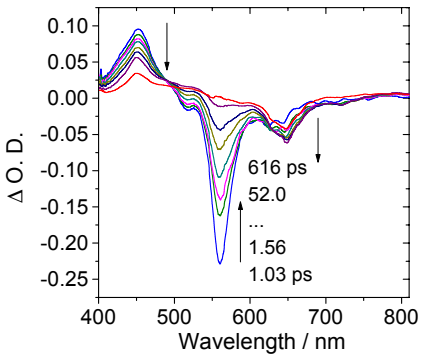

Fig. 9 Femtosecond time-resolved transient absorption spectra of **R-1** upon excitation 555 nm wavelength in DCM.

absorbance at 450 nm, 560 nm and 640 nm (Fig. 9 and Fig. S44). The decrease of the transient absorption at 450 nm and the bleaching band at 560 nm were companied by the development of the transient at 640 nm. Rate constants of 6.70×10^{11} s^{-1} was obtained for the decay of the bleaching band at 560 nm.

In order to observe triplet formation of iodo-styryl-Bodipy units, 640 nm pump pulses were used. Triplet state formation of iodo-styryl-Bodipy units in **R-1** and **R-2** were observed around 1000 ps and 300 ps time delays, respectively (see ESI† Fig S48 S49). Observed triplet state formation times are another indications of ISC rate differences of both compounds. In order to obtain deep insight about ISC rates, decay components of bleach signals around 640 nm for both compounds were compared upon photoexcitation at 640 nm. **R-2** has faster decay component when compared to **R-1** (ESI, Fig S46) indicating different ISC rates.

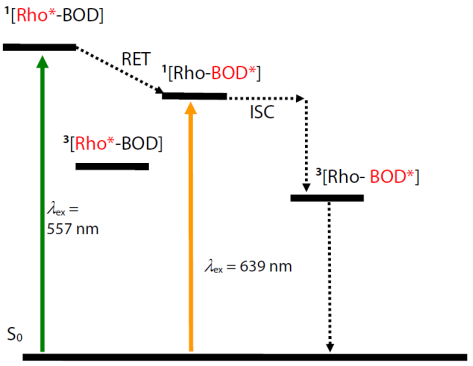

Scheme 2. Qualitative Jablonski energy diagram of the photophysical processes involved in dyad triplet photosensitizer **R-1**. RET stands for resonance energy transfer and ISC stands for intersystem crossing, Rho stands for Rhodamine moiety and BOD stands for iodo Styryl Bodipy part.

The photophysical processes involved in **R-1** and **R-2** with photoexcitation can be summarized in Scheme 2. The two chromophores in **R-1** give absorption at different wavelength, thus broadband absorption was observed. Moreover, the energy level of the S_1 state of Rhodamine part is higher than the styryl Bodipy part (by the fluorescence emission wavelength and the absorption wavelength), thus RET from the Rhodamine part to the iodo-styryl Bodipy is ensured. Due to the lack of heavy atoms on Rhodamine part and the fast efficient RET, population of the T_1 state of the Rhodamine part is neglectable. The T_1 state of the iodo styryl Bodipy was produced due to the heavy atom effect. This state is with lower energy level than the T_1 state of Rhodamine, thus the T_1 state of the dyad is localized on the iodo-styryl Bodipy part, which is confirmed by the nanosecond transient absorption spectra and the DFT calculations on the spin density surfaces (Fig. 7 and Fig. 8).

Singlet oxygen ($^1O_2$) photosensitizing ability

To verify the efficiency of the triplet state yields of the dyad triplet photosensitizers **R-1** and **R-2**, the singlet oxygen ($^1O_2$) quantum yields (Φ_Δ) of the dyad triplet photosensitizers were studied.[8,25,35,66] With selective photoexcitation at the energy donor absorbance (557 nm), Φ_Δ values of 73.8% and 39.6 % were observed for **R-1** and **R-2**, respectively. These values are comparable to the reference compounds **B-1** and **B-2** (Φ_Δ = 62.4% and 58.5 %, respectively). The lower Φ_Δ value of **R-2** (or **B-2**) than **R-1** (or **B-1**) may be due to the more significant intramolecular charge transfer feature of the dimethylaminostyryl moiety in **R-2** (or **B-2**), which may quench the triplet excited state.

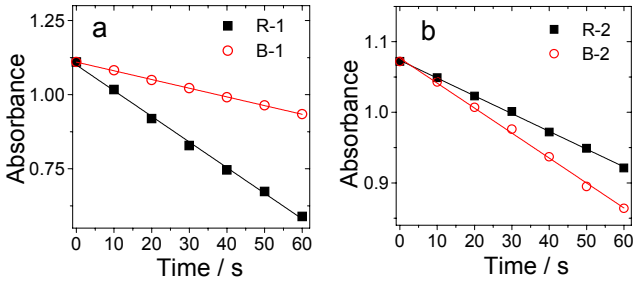

Fig. 10 Singlet oxygen ($^1O_2$) generation with photoexcitation at the absorption of the energy donor of the dyad triplet photosensitizers. Absorbance decrease of **DPBF** with increasing photoirradiation time in the presence of photosensitizers. (a) **R-1** and **B-1**. (b) **R-2** and **B-2**. λ_{ex} = 557 nm, $c = 1.0 \times 10^{-5}$ M in CH_2Cl_2, 20 °C. Deeper slop indicates more efficient $^1O_2$ photosensitizing ability.

The effect of intramolecular energy transfer on the kinetics of $^1O_2$ production with different triplet photosensitizers were presented in Fig. 10 (the energy donor was selectively photoexcited). **R-1** is more efficient to produce $^1O_2$ as compared with that of **B-1**, with excitation at 557 nm, where the energy donor rhodamine absorbs. However, the $^1O_2$ production efficiency of **R-2** is lower than that of **B-2**, indicating that the energy transfer in **R-2** is less efficient.

Photoredox catalytic organic reaction

The triplet photosensitizers were also used for photoredox catalytic organic reactions.[12–14,67,68] One of the major challenge in the area of photoredox catalytic organic reactions is the limited availability of the triplet photosensitizers, i.e. the photocatalysts. The most popular photocatalyst are the Ru(II) complexes, such as $Ru(bpy)_3Cl_2$, $Ir(ppy)_3$, Eosin Y and Rose Bengal. Tailor designed triplet photosensitizer with tunable photophysical properties are highly desired, but were rarely reported. Recently we used iodo-Bodipy,[26] or C_{60}-Bodipy derivatives for photoredox catalytic organic reactions.[25,27] However, these photocatalysts are still

Journal of Materials Chemistry C Accepted Manuscript

suffered from the limitation of mono visible light-harvesting chromophore profile. Since **R-1** and **R-2** show broadband absorption, these compounds are used as photocatalysts for photoredox catalytic organic reaction. Herein we selected the oxidation/[3+2] cycloaddition–oxidative aromatization sequence to construct pyrrolo[2,1-*a*]isoquinolines (via electron transfer mechanism), which are the important skeleton of bioactive natural products.[25,69]

Table 3. Oxidation/[3+2] cycloaddition/aromatization tandem reaction with tetrahydroisoquinolinederivatives catalyzed by organic triplet photosensitizers **R-1, B-1**

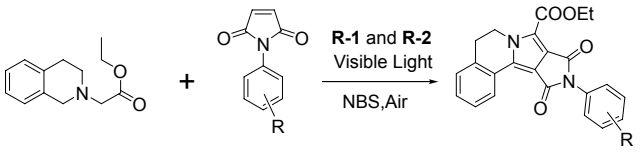

Entry	catalyst [b]	Substrate	Product	t[h] [c]	Yield[d]
1	R-1	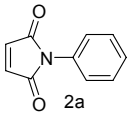	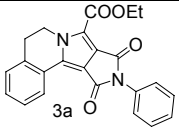	1.5	83%
2	**R-1**	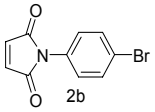	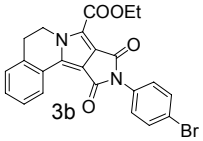	1.5	80%
3	**R-1**	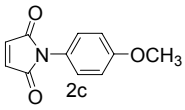	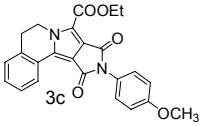	1.5	72%
4	**R-1**	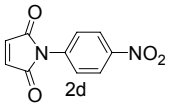	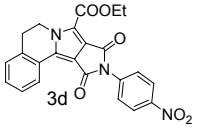	1.5	53%
5	**R-2**	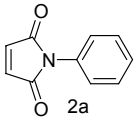	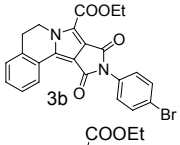	1.5	trace
6[e]	**R-1**	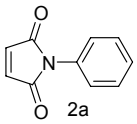	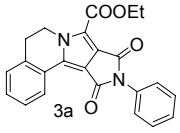	1.5	32%
7[e]	**B-1**	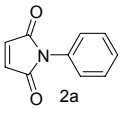	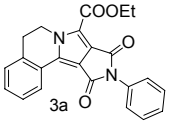	1.5	36%

[a] Reaction conditions: 1 (0.15 mmol), 2 (0.10 mmol), R-1 (2% mol) and NBS (1.2 equiv) were mixed in CH_2Cl_2 (3.0 mL), the mixture was irradiated with 35 W Xe lamp (λ > 385 nm, 300 W/m^2), 20 °C. [b] Catalyst in the reaction. [c] Reaction time with photosensitizers. [d] Yield of isolated products catalyzed with different catalyst. [e] The mixture was irradiated with 35 W Xe lamp (470 > λ > 570 nm,100 mW/cm^2).

Firstly, the reaction conditions were optimized. The results indicated that the DCM is the optimal solvent, and the reaction time is 90 min which is much shorter than the previously reported value of 9 h with the conventional $Ru(bpy)_3Cl_2$ photocatalysts.[69] The enhancement may be due to the strong broadband absorption of the dyad triplet photosensitizers in visible light region. Satisfactory yields were observed for substrates with different electron pushing or electron withdrawing substituents (Table 3).

The mechanism of the photoredox catalytic reactions was studied with ESR (electron spin resonance spectroscopy), with 5,5-dimethyl-1-pyrroline-N-oxide (DMPO) and 2,2,6,6-tetramethylpiperidine (TEMP) as the scavengers for superoxide anion radical ($O_2^{\bullet-}$) and singlet oxygen ($^1O_2$), respectively (see ESI , Fig. S43 and Scheme S1). The results show that the reactions proceed via $O_2^{\bullet-}$. The production of $O_2^{\bullet-}$ is significant in the presence of tetrahydroisoquinoline, whereas the production of $^1O_2$ is completely inhibited in the presence of the tetrahydroisoquinoline substrate.

Intracellular photodynamic studies

It is known that the normal Bodipy and Rhodamine show very weak intersystem crossing (ISC), as a result, these compounds cannot be used as triplet photosensitizers in photocatalysis or the photodynamic therapy (PDT).[1-7,21,24] Instead, the dyad triplet photosensitizers **R-1** and **R-2** show red fluorescence and high singlet oxygen quantum yield (Φ_Δ), thus these compounds can be used as dual-functional materials for luminescence bioimaging as well as PDT studies.

As a preliminary study, the near IR luminescence bioimaging and PDT effect of the dyad photosensitizers **R-1** and **R-2** on a lung cancer cell line of LLC cells were studied (Fig. 11 and Fig. 12). With incubation, the fluorescence microscopy show that the dyad triplet photosensitizers can enter the cytosol. Red fluorescence was observed, which is beneficial for luminescence bioimaging because the long excitation and emissive wavelength can ensure deep penetration of the tissue (Fig. 11).

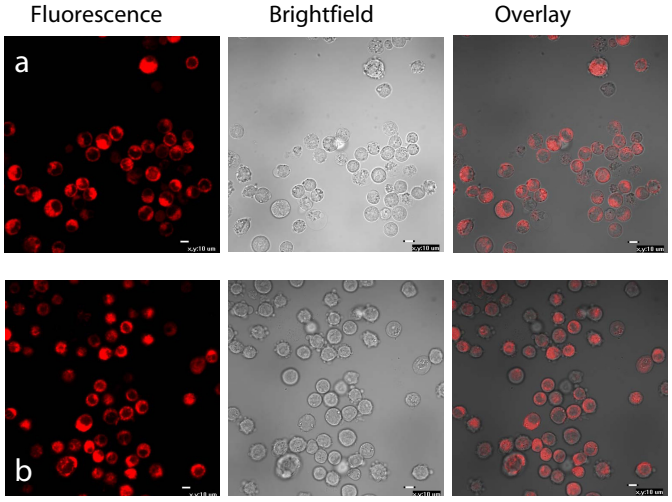

Fig. 11 Confocal fluorescence images in LLC cells (λ_{ex}= 543 nm). The cells were incubated with the photosensitizers (a) **R-1** (b) **R-2** (1.0×10^{-6} M) at 37 °C in the dark for 24 h..

The Rhodamine-Bodipy dyad triplet photosensitizers show high Φ_Δ values (Table 1), strong absorption broadband visible

Journal of Materials Chemistry C Accepted Manuscript

This journal is © The Royal Society of Chemistry [year]

light and long-lived triplet excited state. Therefore, these complexes are used for PDT study (Fig. 12). The LLC cells were incubated with the dyad photosensitizers. Then the cells were irradiated with 635 nm red emitting LED for 4 h. Trypan blue staining of the cells indicated that most of the cells were killed. In a control experiment, however, the cells were not killed without the photosensitizers. These results show that the triplet photosensitizers can be developed as theranostic agents.

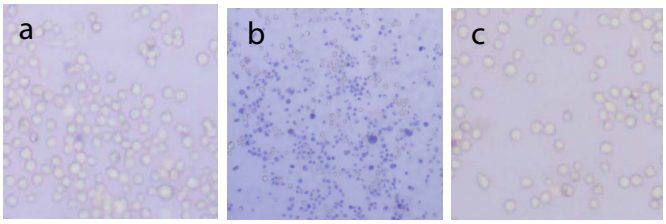

Fig. 12 Photocytotoxic activity of the sensitizers with Trypan blue staining images of LLC cells. (a) cells were incubated with **R-1** and were kept in the dark for 24 h in the same incubator; (b) cells were illuminated with 635 nm LED for 4 h after addition of **R-1** and were incubated for a further 24 h in the dark in the same incubator; (c) cells were illuminated for 4 h without the sensitizers and incubated for another 24 h in the dark in the incubator. The dead cells are preferentially stained with Trypan blue because of increased cellular permeability. The concentration of **R-1** was at 1.0×10^{-6} M. 37 °C.

Conclusions

In summary, we prepared resonance energy transfer (RET)-enhanced organic triplet photosensitizers, which show broadband absorption in visible spectral region. Rhodamine was used as intramolecular energy donor and iodo-styryl-Bodipy was used as energy acceptor and at the same time, the intramolecular spin converter. The two visible light-harvesting chromophores of the dyad gave different absorption wavelength, as a result, the dyad triplet photosensitizers show strong broadband absorption in the visible light region of 450 – 700 nm. The dyad molecular structure protocol of the new triplet photosensitizers is in stark contrast from the conventional triplet photosensitizers. Traditionally the triplet photosensitizers are all based on mono-chormophore profile, resulting in only one major absorption band in the visible spectral region. The photophysical properties of the Rhodamine/iodo-styryl-Bodipy dyad triplet photosensitizers were studied with steady state and nanosecond time-resolved spectroscopy, as well as DFT calculations. Upon excitation at the absorption band of the energy donor (Rhodmaine part), we found that the triplet excited state localized on the iodo-styryl-Bodipy moiety was produced upon visible photoexcitation. The organic triplet photosensitizers were used as photocatalysts and we proved that the dyads triplet photosensitizers are more efficient than the reference triplet photosensitizers that are based on the conventional mono-chromophore profile. The photosensitizers were used for fluorescent staining of cancer cells. Photodynamic therapeutic (PDT) effect was observed. These results show that the triplet photosensitizers can be developed as theranostic agents. Moreover, based on our molecular design methods, it becomes feasible to prepare new organic triplet photosensitizers that show broadband absorption in visible spectral region and predictable ISC. Our results are helpful for designing new organic triplet photosensitizers and for the application of these compounds in photocatalytic organic reactions, photodynamic therapy and for study of the organic photochemistry.

Experimental Section

General Methods

Fluorescence lifetimes were measured with time correlated single photon counting technique (TCSPC) on OB920 spectrometer (Edinburgh instruments, UK). Nanosecond time-resolved transient absorption spectra were measured on LP920 laser flash photolysis spectrometer (Edinburgh Instruments, UK). All the samples in flash photolysis experiments were deaerated with N_2 for ca. 15 min before measurement. The compounds **R-1** and **R-2** were prepared following the reported methods. For preparation of compounds **1**–**3**, see ESI † materials.

Compound 4

Under N_2 atmosphere, a mixture of **3** (1.60 g, 10 mmol) and 2,4-dimethylpyrrole (1.88 g, 20 mmol) in dry CH_2Cl_2 (250 mL) was stirred at rt. On cooling with ice bath, TFA (0.1 mL) was added via syringe. The mixture was stirred overnight at rt. A solution of DDQ (1.13 g, 5 mmol) in THF (30 mL) was added via addition funnel), then the mixture was stirred at rt for 7 h. Triethylamine (15 mL) was added dropwise with cooling on ice bath. The mixture was stirred for another 0.5 h. Then $BF_3{\cdot}Et_2O$ (15 mL) was added dropwise with syringe. The reaction mixture was stirred overnight. The solution was concentrated under reduced pressure. Then water (200 mL) was added, and the mixture was stirred for 24 h. The solution was extracted with CH_2Cl_2 and the organic layer was dried over anhydrous Na_2SO_4. The solvent was evaporated under reduced pressure. The crude product was purified by column chromatography (silica gel, CH_2Cl_2 : hexane = 1:1, v/v) to give **4** as red solid. 600 mg, 16.0 %. ^{1}H NMR (400 MHz, $CDCl_3$) δ 7.21 (d, 2 H, J = 8.0 Hz), 7.10 (d, 2H, J = 8.0 Hz), 5.98 (s, 2H), 4.76 (d, 2H), 2.55 (s, 7H), 1.42 (s, 6H).

Compound 5

4 (250 mg, 0.66 mmol) and *N*-iodosuccinimide (NIS. 468 mg, 2.64 mmol) was dissolved in dry CH_2Cl_2 (50 mL). The mixture was stirred at room temperature. The proceeding of the reaction was monitored by TLC. Then the mixture was concentrated under reduced pressure and the crude product was purified by column chromatography (silica gel. CH_2Cl_2 : hexane = 1:2, v/v). The second band was collected to give the product as a red solid. Yield: 300 mg, 62.0 %. Mp > 250 °C. ^{1}H NMR (400 MHz, $CDCl_3$): δ 7.18–7.11 (m, 4 H), 4.78 (s, 2H), 2.46 (s, 6H), 2.57 (s, 1H), 1.44 (s, 6H). MALDI-HRMS: calcd ($[C_{22}H_{19}BF_2I_2N_2O]^+$) m/z = 629.9648, found m/z = 629.9628.

Compound 6

Under Ar atmosphere, **5** (90.0 mg, 0.14 mmol), benzaldehyde (60.0 mg, 0.56 mmol), acetic acid (3 drops) and piperidine (3 drops) were dissolved in dry DMF (5 mL). Then the resulting solution was subjected to microwave irradiation (5 min, 150 °C, 1 min prestirring). After washing with water, the mixture was purified by column chromatography (silica gel, CH_2Cl_2: PE = 1: 4, v/v) to give a dark solid. Yield: 45.0 mg (40.0%). Mp > 250 °C. ^{1}H NMR (400 MHz, $CDCl_3$): δ 8.18(d, 2H, J = 20.0 Hz), 7.73 (s, 1H), 7.68 (d, 4H, J = 8.0 Hz), 7.43 (t, 4H, J = 8.0 Hz),

Journal of Materials Chemistry C Accepted Manuscript

7.38–7.34 (m, 2H),7.22 (d, 3H, J = 8.0 Hz), 7.15 (d, 2H, J = 8.0 Hz), 4.80 (s, 2H), 2.59 (s, 1H), 1.51 (s, 6H). MALDI-HRMS: *m/z* calcd for $[C_{36}H_{27}N_2OBF_2I_2]^+$ 806.0274; found: 806.0278.

Compound B-2

Under Ar atmosphere, the mixture of **5** (90.0 mg, 0.14 mmol), *p*-*N*,*N*-dimethylamino-benzaldehyde (83.4 mg, 0.56 mmol), acetic acid (3 drops) and piperidine (3 drops) was dissolved in dry DMF (5 mL). The mixture was subjected to microwave irradiation (5 min, 150 °C, 1 min stirring before reaction). After washing with water, the mixture was purified by column chromatography (silica gel, CH_2Cl_2: PE = 1: 1, v/v) to give a dark solid. Yield: 35.0 mg (32.9 %). Mp > 250 °C. ^{1}H NMR (400 MHz, $CDCl_3$): δ 8.19 (s, 1H, J = 16.0 Hz), 7.60–7.51 (m, 3H), 7.26 (m, 2H), 7.20 (d, 2H, J = 12. 0 Hz), 7.13 (d, 2H, J = 8.0 Hz), 4.79 (s, 2H), 3.07 (s, 6H), 2.68 (s, 3H), 2.58 (s, 1H), 1.49 (s, 3H), 1.44 (s, 3H). MALDI-HRMS: *m/z* calcd for $[C_{31}H_{28}N_3OBF_2I_2]^+$ 761.0361; found: 761.0383.

Compound R-0

A mixture of **2** (570 mg, 3 mmol), 3-(diethylamino)phenol (990 mg, 6 mmol), *p*-TsOH (78 mg, 0.45 mmol) and acetic acid (15 mL) was heated at 70 °C and stirred for 7 h. The reaction mixture was cooled to r.t., and the pH was adjusted to above 7.0 with 10% NaOH solution. The precipitate was filtered and washed with water (30 mL). The solid was dissolved in CH_2Cl_2 (30 mL), to which chloranil (366 mg, 1.5 mmol) was added. The mixture was stirred for 2 h. After removal of the solvent, the residue was purified by column chromatography (silica gel; CH_2Cl_2/methanol, 20:1, v/v) to give a purple solid. Yield: 500 mg (34.5 %). ^{1}H NMR (400 MHz, $CDCl_3$): δ 7.45(d, 2H, J = 12.0 Hz), 7.36 (d, 2H, J = 12.0 Hz), 7.21 (d, 2H, J = 12.0 Hz), 6.94–6.91(m, 2H), 6.78 (s, 2H), 4.33 (t, 2H, J = 8.0 Hz), 3.71(t, 2H, J = 8.0 Hz), 3.67–3.61 (m, 8H), 1.32 (t, 12H, J = 8.0 Hz). ^{13}C NMR (100 MHz, $CDCl_3$): 159.95, 157.83, 157.30, 155.23, 132.11, 131.24, 124.04, 115.08, 114.19, 113.96, 113.14, 96.24, 67.39, 50.05, 46.01, 12.55. H RMS (ESI): *m/z* ($[C_{29}H_{34}N_5O_2]^+$) *m/z* = 484.2707, found *m/z* = 484.2705.

Compound R-1

Under Ar atmosphere, **R-0** (24.2 mg, 0.05 mmol) and **6** (32.0 mg, 0.05 mmol) were dissolved in the mixed solvent (14 mL, $CHCl_3$:EtOH:H_2O = 12:1:1, v/v). Then $CuSO_4{\cdot}5H_2O$ (1.5 mg) and sodium ascorbate (2.4 mg) was added. The resulting mixture was stirred at rt for 24 h. Then the reaction mixture was washed with brine and extracted with CH_2Cl_2. Organic layer was dried over anhydrous Na_2SO_4 and evaporated under reduced pressure. The crude product was purified by column chromatography (silica gel, CH_2Cl_2 : CH_3OH = 8 : 1, v/v) to give purple solid. Yield: 32.0 mg, 49.6%. ^{1}H NMR (400 MHz, $CDCl_3$): δ 8.41 (s, 1H), 8.14 (2H, d, J = 16.0 Hz), 7.70 (s, 1H), 7.66 (d, 4H, J = 8.0 Hz), 7.52–7.47 (m, 2H), 7.44–7.41 (m, 4H), 7.35 (d, 4H, J = 8.0 Hz), 7.23 (s, 3H), 7.19–7.13 (m, 4H), 6.96 (s, 2H), 6.76 (s, 2H), 5.33 (s, 2H), 5.01 (s, 2H), 4.72 (s, 2H), 3.64–3.58 (m, 8H), 1.49 (s, 6H), 1.33(t, 12H, J = 4.0 Hz). ^{13}C NMR (100 MHz, $CDCl_3$): 159.99, 159.56, 158.03, 157.61, 155.41, 150.34, 146.31, 139.46, 136.64, 133.42, 132.45, 131.56, 129.47, 128.89, 127.70, 124.33, 118.84, 116.09, 115.45, 114.14, 113.34, 96.39, 66.96, 62.03, 49.76, 46.14, 17.75, 12.74. H RMS (ESI): *m/z* calcd for $[C_{65}H_{61}N_7O_3BF_2I_2]^+$ 1290.2957; found: 1290.2987.

Compound R-2

Under Ar atmosphere, **R-0** (29.0 mg, 0.06 mmol) and **7** (45 mg, 0.06 mmol) were dissolved in the mixed solvent (14 mL, $CHCl_3$: MeOH: H_2O = 12: 1: 1, v/v) then $CuSO_4{\cdot}5H_2O$ (1.5 mg) and sodium ascorbate (2.4 mg) were added. The resulting mixture was stirred at rt for 24 h. Then the reaction mixture was washed with brine and extracted with CH_2Cl_2. The organic layer was dried over Na_2SO_4. The solvent was evaporated under reduced pressure. The crude product was purified by column chromatography to give purple solid. Yield: 40.0 mg (53.5 %) (silica gel, $CHCl_3$: CH_3OH = 8 : 1, v/v). ^{1}H NMR (400 MHz, $CDCl_3$): δ 8.35 (s, 1H), 8.17 (1H, d, J = 16.0 Hz), 7.56–7.46 (m, 6H), 7.34 (d, 2H, J = 8.0 Hz), 7.23 (d, 2H, J = 8.0 Hz), 7.16–7.10 (m, 4H), 6.96 (d, 2H, J = 8.0 Hz), 6.83 (s, 2H), 6.76 (s, 2H), 5.30 (s, 2H), 4.99 (s, 2H), 4.69 (s, 2H), 3.65–3.60 (m, 8H), 3.06 (s, 6H), 2.65 (s, 3H), 1.45 (s, 3H), 1.41 (s, 3H), 1.33(m, 12H). ^{13}C NMR (100 MHz, $CDCl_3$): 160.05, 159.37, 158.09, 157.65, 155.45, 151.47, 151.26, 146.68, 143.36, 140.33, 139.00, 132.41, 131.60, 129.51, 128.94, 127.55, 125.08, 124.36, 115.95, 115.49, 114.18, 113.39, 112.38, 96.43, 67.02, 62.07, 49.95, 46.21, 40.34, 29.81, 17.87, 17.10, 12.80. HRMS (ESI): m/z calcd for $[C_{60}H_{62}N_8O_3BF_2I_2]^+$ 1245.3062; found: 1245.3096.

DFT calucaltions

The density functional theory (DFT) calculations were used for optimization of the ground state geometries, for both singlet states and triplet states. The energy level of the T_1 state (energy gap between S_0 state and T_1 state) were calculated with the time-dependent DFT (TDDFT), based on the ground state geometry. These TDDFT calculations were used for the prediction of the UV-Vis absorption of the T_1 state of the organic triplet photosensitizers, in our case it is the transient absorption of the organic triplet photosensitizers after the laser flash. All the calculations were performed with Gaussian 09.[70]

Femtosecond transient difference absorption spectroscopy.

The ultrafast wavelength dependent pump probe spectroscopy measurements were performed using a Ti:Sapphire laser amplifier-optical parametric amplifier system (Spectra Physics, Spitfire Pro XP, TOPAS) and commercial setup (Spectra Physics, Helios). Pulse duration was measured as 100 fs. Wavelengths of the pump beam were chosen according to the absorption spectra of Rhodamine unit as 555 nm and iodo-styryl-Bodipy unit as 640 nm for **R-1** and **R-2** compounds. White light continuum was used as a probe beam.

Singlet oxygen quantum yield (Φ_Δ)

The $^1O_2$ quantum yields (Φ_Δ) of the photosensitizers were measured with Methylene Blue trihydrate (MB) as standard (Φ_Δ = 0.57 in DCM) and **B-0** as standard (Φ_Δ= 0.83).[71] The absorbance of 1,3-diphenylisobenzofuran (DPBF. $^1O_2$ scavenger) was adjusted around 1.0 in air saturated dichloromethane. Then, the photosensitizer was added to cuvette and photosensitizer's absorbance was adjusted around 0.2–0.3. The cuvette was irradiated with monochromatic light at the peak absorption wavelength for 10 seconds. Absorbance was measured for several times after each irradiation. The slope of absorbance maxima of

Journal of Materials Chemistry C Accepted Manuscript

This journal is © The Royal Society of Chemistry [year]

DPBF at 414 nm versus time graph for each photosensitizer were calculated. Singlet oxygen quantum yield (Φ_Δ) were calculated according to a modified equation:

$$\Phi_\Delta^{bod} = \Phi_\Delta^{ref} \times \frac{k_{bod}}{k_{ref}} \times \frac{F_{ref}}{F_{bod}} \quad \textbf{Eq. 1}$$

where 'bod' and 'ref' designate the photosensitizers and 'MB' respectively. *k* is the slope of difference in change in absorbance of DPBF (414 nm) with the irradiation time, F is the absorption correction factor, which is given by $F = 1-10^{-O.D.}$ (O.D. is the optical density of the solution at the irradiation wavelength).

Cell Culture

LLC cells (lung cancer cell) were grown in RPMI-1640 Medium in an atmosphere of 5% CO_2, 95% air at 37 °C supplemented with 10% fetal bovine serum (FBS), and 1% antibiotics (penicillin /streptomycin, 100 U/mL).

Laser scanning Confocal fluorescence microscope

Fluorescent images were acquired on Nikon ECLIPSE-Ti confocal laser scanning microscopy. The excitation wavelength was 543 nm. Cell imaging was carried out in confocal Petri dishes.

Photodynamic therapy experiment

The DMSO solution of **R-1** and **R-2** was added to 2000 μL cell suspensions in RPMI-1640 medium and keep the final concentration at 1.0×10^{-6} M. Trypan blue was used to stain the dead cells because of increased cellular permeability. All the staining measurements were carried out within 5 min, after 0.4% Trypan blue dyes solution was added.

To evaluate the triplet photosensitizers' cytotoxicity, LLC cells were incubated with triplet photosensitizers and were kept in the dark for 24 h in the same incubator. To identify the cytotoxicity of sensitizers, cells were illuminated with 635 nm LED for 4 h after addition of the triplet photosensitizers and were incubated for another 24 h in the dark in the same incubator. As control, cells were illuminated for 4 h without the triplet photosensitizers and incubated for another 24 h in the dark. All the measurements were carried out in triplicate.

Acknowledgement

We thank the NSFC (20972024, 21073028 and 21273028), the Royal Society (UK) and NSFC (China-UK Cost-Share Science Networks, 21011130154), Science Foundation Ireland (SFI E.T.S. Walton Program 11/W.1/E2061) and Ministry of Education (NCET-08-0077 and SRFDP-20120041130005) for financial support.

Notes and references

[a] *State Key Laboratory of Fine Chemical, School of Chemical Engineering, Dalian University of Technology, Dalian, 116024, P.R. China. Fax: (+86) 411-8498-6236; E-mail: zhaojzh@dlut.edu.cn; Group homepage: http://finechem.dlut.edu.cn/photochem;*

[b] *College of Chemistry and Chemical Engineering, Qiqihaer University, Qiqihaer 161006, Heilongjiang, P. R. China;*

[c] *Center Laboratory, Affiliated Zhongshan Hospital of Dalian University, Dalian 116001, P. R. China;*

[d] *Department of Engineering Physics, Faculty of Engineering, Ankara University, 06100 Beşevler, Ankara, Turkey;*

[e] *Department of Chemistry, Faculty of Science, Ankara University, 06100 Beşevler, Ankara, Turkey. E-mail: hayvali@science.ankara.edu.tr*

‡ These authors contribute equally to the work.

Contribution of the authors: J. Ma carried out the preparation of the compounds and the spectroscopy studies; X. Yuan, S. Li and X. Li did the studies on cellular imaging, Caishun Zhang contributes to the synthesis of some intermediate compounds; P. Majumdar helped in the spectroscopy and cellular studies; J. Zhao is responsible for the research, Ahmet Karatay and Betül Küçüköz conducted pump-probe experiments together. Ayhan Elmali, H. Gul Yaglioglu, and Mustafa Hayvali are responsible for the femto-second spectroscopy studies.

† Electronic Supplementary Information (ESI) available: molecular structure characterization data, UV/Vis absorption and emission spectra, time-resolved transient absorption spectroscopy and DFT calculations. See DOI: 10.1039/b000000x/

1 A. Gorman, J. Killoran, C. O'Shea, T. Kenna, W. M. Gallagher and D. F. O'Shea, *J. Am. Chem. Soc.*, 2004, **126**, 10619–10631.
2 T. Yogo, Y. Urano, Y. Ishitsuka, F. Maniwa, and T. Nagano, *J. Am. Chem. Soc*., 2005, **127**, 12162–12163.
3. N. Adarsh, R. R. Avirah and D. Ramaiah, *Org. Lett.,* 2010, **12**, 5720–5723.
4. Y. Cakmak, S. Kolemen, S. Duman, Y. Dede, Y. Dolen, B. Kilic, Z. Kostereli, L. T. Yildirim, A. L. Dogan, D. Guc and E. U. Akkaya, *Angew. Chem. Int. Ed.*, 2011, **50**, 11937–11941.
5. S. G. Awuah and Y. You, *RSC Adv*., 2012, **2**, 11169–11183.
6. Y. Yang, Q. Guo, H. Chen, Z. Zhou, Z. Guo and Z. Shen, *Chem. Commun.,* 2013, **49**, 3940–3942.
7. J. Zhao, W. Wu, J. Sun and S. Guo, *Chem. Soc. Rev.,* 2013, **42**, 5323–5351.
8. S.Takizawa, R. Aboshi and S. Murata, *Photochem. Photobiol. Sci.*, 2011, **10**, 895–903.
9. (*a*) R. B. P. Elmes, M. Erby, S. M. Cloonan, S. J. Quinn, D. C. Williams and T. Gunnlaugsson, *Chem. Commun.,* 2011, **47**, 686–688; (*b*) S. Banerjee, J. A. Kitchen, S. A. Bright, J. E. O'Brien, D. Clive Williams, J. M. Kelly and T. Gunnlaugsson. *Chem. Commun.*, 2013, **49**, 8522–8524; (*c*) R. B. P. Elmes, J. A. Kitchen, D. C. Williams, T. Gunnlaugsson. *Dalton Trans.*, 2012, **41**, 6607–6610; (*d*) S. Banerjee, J. A. Kitchen, T. Gunnlaugsson and J. M. Kelly, *Org. Biomol. Chem*., 2013, **11**, 5642–5655; (e) S. Banerjee, E. B. Veale, C. M. Phelan, S. A. Murphy, G. M. Tocci, L. J. Gillespie, D. O. Frimannsson, J. M. Kelly and T. Gunnlaugsson, *Chem. Soc. Rev.*, 2013, **42**, 1601–1618.
10 F. Schmitt, J. Freudenreich, N. P. E. Barry, L. Juillerat-Jeanneret, G. Süss-Fink, and B. Therrien, *J. Am. Chem.Soc*., 2012, **134**, 754−757.
11 J. Xuan and W. -J Xiao. *Angew. Chem. Int. Ed.*, 2012, **51**, 6828–6838.
12 L. Shi and W. Xia, *Chem. Soc. Rev.,* 2012, **41**, 7687–7697.
13 S. Fukuzumi and K. Ohkubo, *Chem. Sci*., 2013, **4**, 561–574.
14 Y. Xi, H. Yi and A. Lei, *Org. Biomol. Chem*., 2013, **11**, 2387–2403.
15 J. W. Tucker and C. R. J. Stephenson, *J. Org. Chem*., 2012, **77**, 1617−1622.
16 F. Gärtner, S. Denurra, S. Losse, A. Neubauer, A. Boddien, A. Gopinathan, A. Spannenberg, H. Junge, S. Lochbrunner, M. Blug, S. Hoch, J. Busse, S. Gladiali, and M. Beller, *Chem. Eur. J.,* 2012, **18**, 3220–3225.
17 W.-G. Wang, F. Wang, H.-Y. Wang, C.-H. Tung and L.-Z. Wu, *Dalton Trans.*, 2012, **41**, 2420–2426.
18 X. Wang, S. Goeb, Z. Ji, N. A. Pogulaichenko, and F. N. Castellano, *Inorg. Chem*., 2011, **50**, 705–707.
19 S. Jasimuddin, T. Yamada, K. Fukuju, J. Otsuki and K. Sakai, *Chem. Commun.,* 2010, **46**, 8466–8468.
20 T. N. Singh-Rachford, F. N. Castellano, *Coord. Chem. Rev.,* 2010, **254**, 2560–2573.

Journal of Materials Chemistry C Accepted Manuscript

21. J. Zhao, S. Ji and H. Guo, *RSC Adv.*, 2011, **1**, 937–950.
22. A. Monguzzi, R. Tubino, S. Hoseinkhani, M. Campione and F. Meinardi, *Phys. Chem. Chem. Phys*., 2012, **14**, 4322–4332.
23. Y. C. Simon and C. Weder, *J. Mater. Chem.*, 2012, **22**, 20817–20830.
24. A. Kamkaew, S. H. Lim, H. B. Lee, L. V. Kiew, L. Y. Chung and K. Burgess, *Chem. Soc. Rev.,* 2013, **42**, 77–88.
25. L. Huang and J. Zhao, *Chem. Commun.,* 2013, **49**, 3751–3753.
26. L. Huang, J. Zhao, S. Guo, C. Zhang, and J. Ma, *J. Org. Chem*., 2013, **78**, 5627−5637.
27. L. Huang, X. Yu, W. Wu, and J. Zhao, *Org. Lett*., 2012, **14**, 2594−2597.
28. W. Wu, J. Zhao, J. Sun, and S. Guo, *J. Org. Chem*., 2012, **77**, 5305−5312.
29. (*a*) C. Zhang, J. Zhao, S. Wu, Z. Wang, W. Wu, J. Ma, S. Guo, and L. Huang, *J. Am. Chem. Soc*., 2013, **135**, 10566−10578; (*b*) S. Guo, L. Ma, J. Zhao, B. Küçüköz, A. Karatay, M. Hayvali, H. Gul Yaglioglu and A. Elmali, *Chem. Sci.*, 2014, **5**, 489–500; (*c*) L. Huang, X. Cui, B. Therrien, and J. Zhao, *Chem. Eur. J.* 2013, **19**, 17472–17482.
30. J. Fan, M. Hu, P. Zhan and X. Peng, *Chem. Soc. Rev.,* 2013, **42**, 29−43.
31. G. Chen, F. Song, J. Wang, Z. Yang, S. Sun, J. Fan, X. Qiang, X. Wang, B. Dou and X. Peng, *Chem. Commun*., 2012, **48**, 2949–2951.
32 M. H. Lee, J. H. Han, J. H. Lee, N. Park, R. Kumar, Ch. Kang, and J. S. Kim, *Angew. Chem. Int. Ed*., 2013, **52**, 6206–6209.
33 (*a*) H. Yu, Y. Xiao, H. Guo, and X. Qian, *Chem. Eur. J.,* 2011, **17**, 3179 – 3191; (*b*) C. Bonnier, D. D. Machin, O. Abdia and B. D. Koivisto, *Org. Biomol. Chem*., 2013, **11**, 3756–3760; (*c*) J. M. Serin, D. W. Brousmiche, J. M. J. Fréchet, *J. Am. Chem. Soc.* 2002, **124**, 11848–11849.
34 L. Huang, L. Zeng, H. Guo, W. Wu, W. Wu, S. Ji, and J. Zhao, *Eur. J. Inorg. Chem.,* **2011**, 4527–4533.
35 N. Adarsh, M. Shanmugasundaram, R. R. Avirah, and D. Ramaiah, *Chem. Eur. J.,* 2012, **18**, 12655–12662.
36 (*a*) Y. Chen, J. Zhao, L. Xie, H. Guo and Q. Li, *RSC Adv.*, 2012, **2**, 3942–3953; (*b*) W. Wu, H. Guo, W. Wu, S. Ji, and J. Zhao, *J. Org. Chem*., 2011, **76**, 7056–7064; (*c*) M. Nakamura, H. Tahara, K. Takahashi, T. Nagata, H. Uoyama, D. Kuzuhara, S. Mori, T. Okujima, H. Yamadad and H. Uno. *Org. Biomol. Chem.*, 2012, **10**, 6840–6849; (*d*) S. Zhang, T. Wu, J. Fan, Z. Li, N. Jiang, J. Wang, B. Dou, S. Sun, F. Songa and X. Peng, *Org. Biomol. Chem.*, 2013, **11**, 555–558; (*e*) H. Pan, G.-L. Fu, Y.-H. Zhao, C.-H. Zhao, *Org. Lett.*, 2011, **13**, 4830–4833; (*f*) G.-L. Fu, H.-Y. Zhang, Y.-Q. Yan, C.-H. Zhao, *J. Org. Chem.*, 2012, **77**, 1983−1990.
37 (*a*) X. Jia, X. Yu, X. Yang, J. Cui, X. Tang, W. Liu, W. Qin, *Dyes and Pigms* 2013, **98**, 195–200; (*b*) N. Boens; V. Leen, W. Dehaen, L. Wang, K. Robeyns, W. Qin, X. Tang, D. Beljonne, C. Tonnele, *J. Phy. Chem. A*, 2012, **116**, 9621–9631; (*c*) D. Kand, P. K. Mishra, T. Saha, M. Lahiri and P. Talukdar. *Analyst*, 2012, **137**, 3921–3924; (*d*) B. Brizet, C. Bernhard, Y. Volkova, Y. Rousselin, P. D. Harvey, C. Goze and F. Denat, *Org. Biomol. Chem.*, 2013, **11**, 7729–7737; (*e*) S. L. Niu, C. Massif, G. Ulrich, R. Ziessel, P.-Y. Renardbcd and A. Romieu, *Org. Biomol. Chem.*, 2011, **9**, 66–69; (*f*) C. M. Cooley, K. S. Hettie, J. L. Klockow, S. Garrison and T. E. Glass, *Org. Biomol. Chem.*, 2013, **11**, 7387–7392.
38 M. Yuan, X. Yin, H. Zheng, C. Ouyang, Z. Zuo, H. Liu, Y. Li, *Chem. Asian J.,* 2009, **4**, 707–713.
39 M. E. El-Khouly, A. N. Amin, M. E. Zandler, S. Fukuzumi, and F. D'Souza, *Chem. Eur. J*., 2012, **18,** 5239 –5247.
40 Z. Kostereli, T. Ozdemir, O. Buyukcakir, and E. U. Akkaya, *Org. Lett*., 2012, **14**, 3636 –3639.
41 J.-Y. Liu, Y. Huang, R. Menting, B. Röder, E. A. Ermilov and D. K. P. Ng, *Chem. Commun.,* 2013, **49**, 2998–3000.
42 J. Liu, M. E. El-Khouly, S. Fukuzumi, and D. K. P. Ng, *Chem. Asian J.,* 2011, **6**, 174–179.
43 A. Coskun and E. U. Akkaya. *J. Am. Chem. Soc*., 2006, **128**, 14474–14475.
44 J. Shao, H. Sun, H. Guo, S. Ji, J. Zhao, W. Wu, X. Yuan, C. Zhang and T. D. James, *Chem. Sci.*, 2012, **3**, 1049–1061.
45 R. Ziessel, B. D. Allen, D. B. Rewinska, and A. Harriman, *Chem. Eur. J*., 2009, **15**, 7382–7393.
46 R. Ziessel and A. Harriman, *Chem. Commun.,* 2011, **47**, 611–631.
47 N. J. Turro, V. Ramamurthy and J. C. Scaiano, *Principles of Molecular Photochemistry: An Introduction*, University Science Books, Sausalito, CA, 2009.
48 P. A. Hal, J. Knol, B. M. W. Langeveld-Voss, S. C. J. Meskers, J. C. Hummelen, and R. A. J. Janssen, *J. Phys. Chem. A*, 2000**, 104***,* 5974–5988.
49 C. C. Hofmann, S. M. Lindner, M. Ruppert, A. Hirsch, S. A. Haque, M. Thelakkat, and J. Köhler, *J. Phys. Chem. B,* 2010**, 114***,* 9148–9156.
50 A. N. Amin, M. E. El-Khouly, N. K. Subbaiyan, M. E. Zandler, S. Fukuzumi and F. D'Souza, *Chem. Commun.,* 2012, **48**, 206–208.
51 M. Lindgren, B. Minaev, E. Glimsdal, R. Vestberg, R. Westlund and E. Malmström, *J. Lumin.*, 2007, **124,** 302–310.
52 B. F. Minaev, G. V. Baryshnikov, V. A. Minaeva. *Dyes Pigm.*, 2011, **92**, 531–536.
53 B. Minaev, H. Aren, F. D. Angelis, *Chem. Phys., 2*009, **358**, 245–257.
54 K. Hanson, Arnold Tamayo, Vyacheslav V. Diev, Matthew T. Whited, Peter I. Djurovich and M. E. Thompson, *Inorg. Chem.,* 2010, **49**, 6077–6084.
55 J. Zhao, S. Ji, W. Wu, W. Wu, H. Guo, J. Sun, H. Sun, Y. Liu, Q. Li and L. Huang, *RSC Adv*., 2012, **2**, 1712–1728.
56 W. Wu, J. Sun, S. Ji, W. Wu, J. Zhao and Huimin Guo, *Dalton Trans*., 2011, **40**, 11550–11561.
57 P. Yang, W. Wu, J. Zhao, D. Huang and X. Yi, *J. Mater. Chem*., 2012, **22**, 20273–20283.
58 D. Huang, J. Sun, L. Ma, C. Zhang and J. Zhao, *Photochem. Photobiol*. Sci., 2013, **12**, 872−882.
59 S. Guo, J. Sun, L. Ma, W. You, P. Yang and J. Zhao, *Dyes Pigm.*, 2013, **96**, 449–458.
60 Y. Chen, J. Zhao, H. Guo, and L. Xie, *J. Org. Chem*. 2012, **77**, 2192−2206.
61 H. Guo, Y. Jing, X. Yuan, S. Ji, J. Zhao, X. Li and Y. Kan, *Org. Biomol. Chem.*, 2011, **9**, 3844–3853.
62 S. Ji, J. Yang, Q. Yang, S. Liu, M. Chen, and J. Zhao, *J. Org. Chem.* 2009, **74**, 4855–4865.
63 D. Kand, A. M. Kalleb and P.Talukdar, *Org. Biomol. Chem*., 2013, **11**, 1691–1701.
64 D. Kand, P. K. Mishra, T. Saha, M. Lahiri and P. Talukdar, *Analyst*, 2012, **137,** 3921–3924.
65 D. Setiawan, A. Kazaryan, M. A. Martoprawirob and M. Filatov, *Phys. Chem. Chem. Phys.*, 2010, **12**, 11238–11244.
66 J. Sun, J. Zhao, H. Guo and W. Wu, *Chem. Commun*., 2012, **48**, 4169–4171.
67 J. M. R. Narayanam and C. R. J. Stephenson, *Chem. Soc. Rev*., 2011, **40**, 102–113.
68 D. Ravelli, M. Fagnoni and A. Albini, *Chem. Soc. Rev.,* 2013, **42**, 97–113.
69 Y.-Q. Zou, L.-Q. Lu, L. Fu, N.-J. Chang, J. Rong, J.-R. Chen and W.-J. Xiao, *Angew. Chem. Int. Ed.* 2011, **50**, 7171 –7175.
70 M. J. Frisch, et al., *Gaussian 09*, *Revision 01*, Gaussian Inc., Wallingford, CT, 2009.
71 W. Li, L. Li, H. Xiao, R. Qi, Y. Huang, Z. Xie, X. Jing and H. Zhang. *RSC Adv.*, 2013, **3**, 13417–13421.

This journal is © The Royal Society of Chemistry [year]

Journal of Materials Chemistry C Accepted Manuscript

Graphical contents entry:

Resonance energy transfer-enhanced rhodamine-styryl bodipy dyad triplet photosensitizers

Jie Ma,[a,b‡] Xiaolin Yuan,[c‡] Betül Küçüköz,[d] Shengfu Li,[c] Caishun Zhang,[a] Poulomi Majumdar,[a] Ahmet Karatay,[d] Xiaohuan Li,[c] H. Gul Yaglioglu,[d] Ayhan Elmali,[d] Jianzhang Zhao[a]* and Mustafa Hayvali [e]*

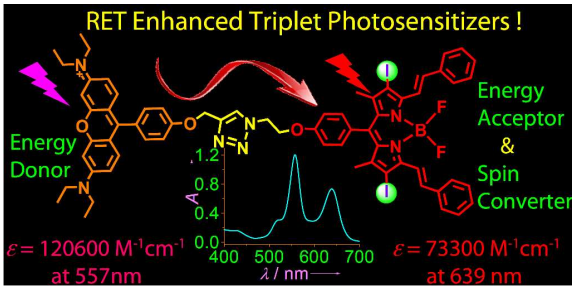

Broadband visible light-absorbing triplet photosensitizers with Rhodamine as energy donor and styryl Bodipy as energy acceptor/spin converter were prepared.

Keyword: Bodipy, photochemistry, Rhodamine, Triplet photosensitizer, Resonance energy transfer

Journal of Materials Chemistry C Accepted Manuscript